SOIL SCIENCE

Thermal monitoring of a Cryosol in a high marine terrace (Half Moon Island, Maritime Antarctica)

CARLOS ERNESTO G.R. SCHAEFER, MÁRCIO R. FRANCELINO, ANTONIO B. PEREIRA, ROBERTO F.M. MICHEL, DANIELA SCHMITZ, IORRANA F. SACRAMENTO, WILLIAM F. RODRIGUES & CAIK O. DE MIRANDA

Abstract: Active layer and permafrost are important indicators of climate changes in periglacial areas of Antarctica, and the soil thermal regime of Maritime Antarctica is sensitive to the current warming trend. This research aimed to characterize the active layer thermal regime of a patterned ground located at an upper marine terrace in Half Moon Island, during 2015-2018. Temperature and moisture sensors were installed at different soil depths, combined with air temperature, collecting hourly data. Statistical analysis was applied to describe the soil thermal regime and estimate active layer thickness. The thermal regime of the studied soil was typical of periglacial environment, with high variability in temperature and water content in the summer, resulting in frequent freeze-thaw cycles. We detected dominant freezing conditions, whereas soil temperatures increased, and the period of high soil moisture content lasted longer over the years. Active layer thickness varied between the years, reaching a maximum depth in 2018. Permafrost degradation affects soil drainage and triggers erosion in the upper marine terrace, where permafrost occurrence is unlikely. Longer monitoring periods are necessary for a detailed understanding on how current climatic and geomorphic conditions affect the unstable permafrost of low-lying areas of Antarctica (marine terraces).

Key words: climate change, holocene terraces, soil moisture, soil thermal regime, permafrost.

INTRODUCTION

In the Antarctic continent, permafrost is mainly found in the ice-free areas located around the continent margins, islands and nunataks (Bockheim 1995, Hrbáček et al. 2018). Permafrost is defined as ground at a temperature equal or lower than 0 °C for a minimum period of two years, where the active layer fluctuates seasonally between positive and negative temperatures (Dobiński 2020). It is very sensitive to climatic changes once it intermediates the heat flux between atmosphere and substrate (Smith 1990). Maritime Antarctic region is more sensitive to short climatic changes than the Antarctic continent due to its greater oceanic influence (Curl 1980), which brings greater effect from sea ice, ocean currents and global ocean circulation. The warmer and wetter conditions, compared to the colder and dryer continent interior, favor the formation of an ice-cemented permafrost (moisture content > 10%, Bockheim & Tarnocai 1998), and the occurrence of more freezing and thawing cycles. However, permafrost is generally absent or degraded on marine terraces (Francelino et al. 2011).

Many studies have pointed to a warming trend of the active layer and permafrost at

the global scale. The Antarctic Peninsula has experienced a major warming over the last 50 years, with temperatures at Faraday/Vernadsky station having increased at a rate of 0.56 °C decade^{-1} over the year and 1.09 °C decade^{-1} during the winter; both figures are statistically significant at less than the 5% level (Turner et al. 2005). Most recent studies in the AP and surrounding islands, such as the South Shetland Islands (SSI), found a shift of this atmospheric warming trend to a cooling trend during 1999–2014 (Turner et al. 2016, Oliva et al. 2017). This cooling trend was observed to be seasonally dependent, being more pronounced during the autumn and winter season, and strongly influenced by the extent and duration of the sea ice (Oliva et al. 2017). This period has led to the thinning of the active layer and even permafrost aggradation at several areas in the SSI (Ramos et al. 2017, 2020).

Beyond its climatic relevance, the active layer controls hydrological, geomorphological and pedological processes, such as frost heaving, sorting, gelifluction and cryoturbation, which can lead to important impacts on periglacial landscapes (López-Martínez et al. 2012). Due to its importance, research has focused on the active layer thermal regime throughout Antarctica, especially in the Antarctica Peninsula, which concentrate most of the monitoring sites of the Circumpolar Active Layer Monitoring program (CALM, Vieira et al. 2010). Many results on the behavior of the active layer thermal regime (ALTR) have been published (Almeida et al. 2014, 2017, Chaves et al. 2017, de Pablo et al. 2013, 2014, Guglielmin et al. 2012, Michel et al. 2012, 2014, Oliva et al. 2017), highlighting changes in the ALTR induced by vegetation (Guglielmin et al. 2014, Hrbáček et al. 2020, Silva et al. 2020), climate (Guglielmin & Cannone 2012, Hrbáček et al. 2016, Wilhelm & Bockhiem 2016), birds

(Schaefer et al. 2017b), landforms (Schaefer et al. 2017a), and substrates (Hrbáček et al. 2016).

In Half Moon Island, located between Livingston and Greenwich Islands in the SSI, the periglacial phenomenon is important, and active processes and landforms are found, with an unusual widespread patterned ground development on upper, older (>10 m a.s.l) marine terrace (>10 m a.s.l) marine terrace (Serrano & López-Martínez 1997). Patterned ground is widespread in the SSI and is generally associated with the presence of permafrost, being one of the most developed and significant features promoted by freezing and thawing cycles (López-Martínez et al. 2012), but it is generally absent on low lying marine terraces (Francelino et al. 2011). Thus, the tiny Half Moon Island represents an interesting site for active layer monitoring since it suffered intense post glacial uplift of Late Holocene marine terraces, without any significant glacier and is located in a very area sensitive area to climate change.

Despite the recent efforts, there is still a lack of information about Antarctic permafrost spatial variability and its thermal dynamic compared to other polar regions (Hrbáček et al. 2018). In this paper, we characterize the active layer thermal regime of an unusual permafrost-affected soil with patterned ground located at the upper marine terrace of Half Moon Island, from 2015 to 2018 period.

MATERIALS AND METHODS
Study area
Half Moon Island (HMI) is a tiny (171 ha) island, lying in the McFarlane Strait, in the SSI. It is located between the latitudes 62°34'50.57"S and 62°35'54.04"S and longitudes of 59°53'24.44"W and 59°56'04.16"W (Figure 1a). It has one of the 13 Argentinian research bases in Antarctica, that served as a permanent base from 1953 to
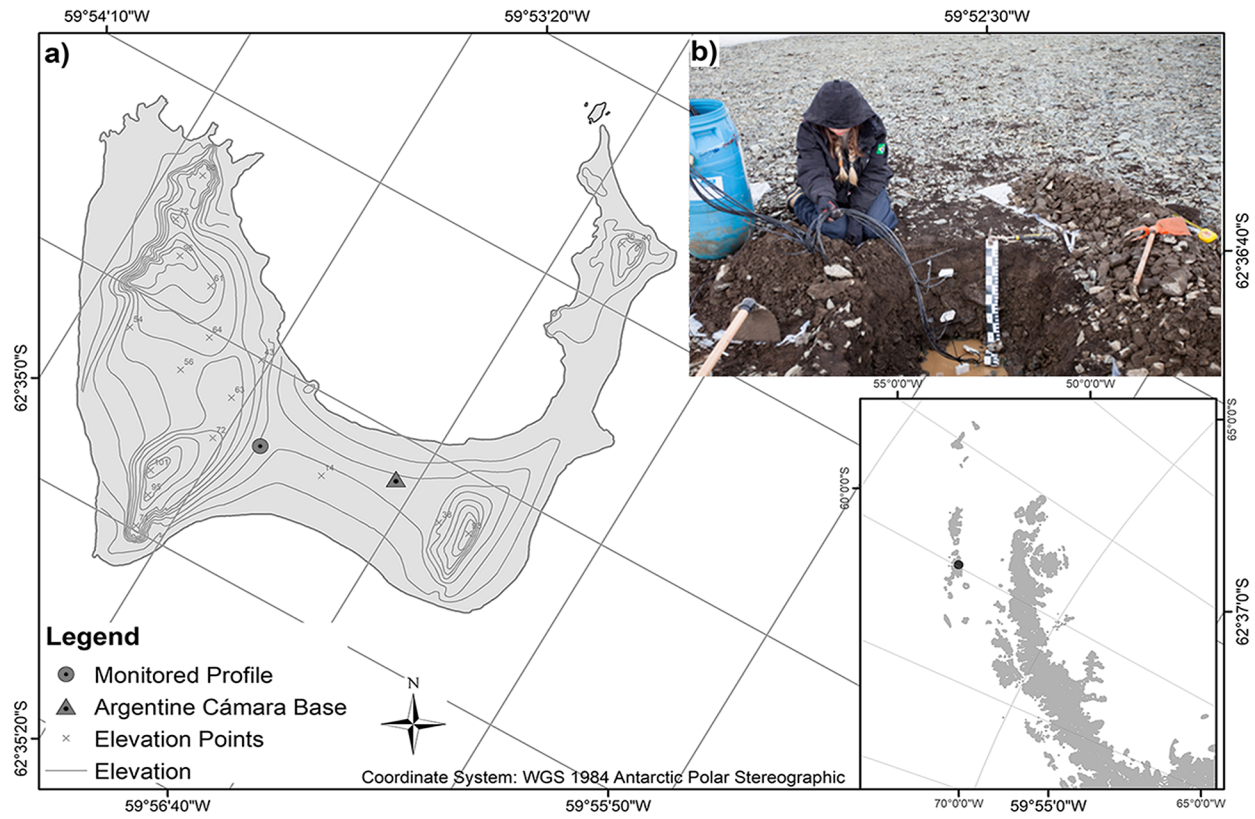
Figure 1. Half Moon Island. a) Local and regional maps; b) Monitored soil profile.

1988, and as a summer season facility since then. The Köppen's classification for the region show a polar (ET) climate. The mean annual air temperature of HMI is near -2 °C and the average summer temperatures are above freezing point, which allow snow cover melting and freezing-thawing cycles. These conditions favor the formation of a shallow lake, at the uppermost marine terrace (16.8 m above the present shore line), with enough water to meet the Argentine Cámara Base demands.

Geologically, the island is mainly composed of andesites and basaltic andesites rocks (Smellie et al. 1984). The island altitude at the northern portion reaches 101 m a.s.l. HMI was formed by the junction of three smaller islands during the Holocene, and is structurally controlled by two rock outcrops on the east and west portions of the island, linked by a tombolo formed by the marine deposition of gravel and

finer sediments near coastlines. This process builds up opposite terraces that developed into a connecting isthmus formed a gravelly uplifted marine terrace with a succession of well-defined raised beaches, which are the result of the glacio-isostatic rebound of the Shetland Islands following the Holocene deglaciation (Fretwell et al. 2010).

Permafrost occurs over wide areas on high Holocene beaches, being sporadic on the lowest present-day platforms (López-Martínez et al. 2012). Landforms related to permafrost, such as patterned ground, are widespread in HMI. They occur on the Holocene uplifted marine terrace, over gently slopes and stable surfaces, and mainly present circular and polygonal forms (Araya & Hervé 1972, Martinez & Massone 1995 López-Martínez et al. 2016, Serrano & López-Martínez 1997). At more elevated terrain, stone stripes, gelifluction sheets and gelifluction

lobes prevail due to slope angle and outcrops of andesite intrusions, which provide raw material enabling the formation of these features (Serrano & López-Martínez 1997).

Penguin rookeries are located mainly on Baliza Point at the east portion of the island. Plant communities comprises a variety of species including bryophytes, lichens, one of the flowering plants (*Deschampsia antartica* Desv.) of Antarctica and terrestrial algae (Schmitz et al. 2018). HMI is one of the main landing locations of the touristic visitation activity in the Shetland Islands during the summer season.

Soil and air temperature monitoring

The active layer and permafrost monitoring site (62°35'23.8" S, 59°55'18.3" W at 44 m of altitude) was installed in the summer of 2015 and consists of five soil temperature sensors (L107E, Campbell Scientific Inc., Utah, USA – accuracy of ± 0.2 °C) arranged vertically in the soil profile down to the bottom of the active layer, at 5 cm, 10 cm, 30 cm, 50 cm and 100 cm depth; four soil moisture content (SMC) sensors (CS656 water content reflectometer, accuracy of ± 2.5%) at 10 cm, 30 cm, 50 cm and 100 cm depth; and one air temperature probe (L107E, Campbell Scientific Inc., Utah, USA – accuracy of ± 0.2 °C) at 1 m above the ground. The system was installed in a Turbic Eutric Cryosol, developed on an uplifted marine terrace deposits with well-developed patterned ground, where angular cobbles also occur and are product of frost transported shattered material along the slope (Figure 1b). Probes were connected to a data logger (model CR1000, Campbell Scientific Inc.), recording data at hourly intervals from March 2015 to December 2018.

Soil samples were collected in respect to the pedological differentiation of horizons for the soil texture analysis. The < 2 mm samples were passed through mechanical dispersion in distilled water, sieving and weighting of the coarse and fine sand, sedimentation of the silt fraction followed by siphoning of the <2 μm fraction (Gee & Bauder 1986). Soil textural classes were determined using a soil textural chart (Coarse Sand 0.2 – < 2 mm, Fine Sand 0.05 –< 0.2 mm, Silt 0.002 – < 0.05 mm and Clay < 0.002 mm).

We calculated the thawing days (days in which all hourly soil temperatures are positive and at least one reading is warmer than 0.5 °C), freezing days (days in which all hourly soil temperature measurements are negative and at least one reading is colder than -0.5 °C), isothermal days (days in which all the hourly measurements range only between ± 0.5 °C, Chambers, 1966), freeze–thaw days (days in which there are both negative and positive temperatures with at least one value higher than 0.5 °C or lower than -0.5 °C), thawing degree days (TDD, obtained by the cumulative sum of the mean daily temperatures above 0 °C) and freezing degree days (FDD, obtained by the cumulative sum of the mean daily temperatures below 0 °C) (Guglielmin et al. 2008). The active layer thickness (ALT) was calculated as the 0 °C depth by using a simple regression function for extrapolating the thermal gradient from the two deepest positive daily averages, for each year separately (Guglielmin 2006).

Statistical analysis was applied to describe soil temperature time series. All statistical procedures were performed using the software R version 4.0.4 (R Core Team 2020). The histograms were created to evaluate the frequency distribution of temperature readings and the time series were decomposed into its remainder, seasonal and trend components, by locally weighted smoothing (Loess) with a window of 25 hours, using the stl package, based on Cleveland et al. (1990).

RESULTS

Soil profile characterization

The profile was classified as a Turbic Eutric Cryosol, according to the World Reference Base for Soil Resources (ISSS 1988). It presented patterned ground at the surface and developed over an abandoned penguin breeding site. Due to the coarse nature of the profile, features such as frost heave and solifluction were not observed; wind erosion was evident. Horizons A, B1 and B2 expressed weak angular block structure, loamy fine sand (A) and sandy loam (B1 and B2) textures and greater silt content, specially B2, that also presented greater clay content (Table I). At 25 cm there was a clear transition from B2 to C, where gravel content increased considerably, and the ornithogenic influence reduced. The texture is still sandy loam, although the percentage of sand increases. At 100 cm a saturated transition layer just above the permafrost table was presented, characterized as Cg horizon, and ice-cemented permafrost was just below it.

Temperature and moisture regimes

The maximum mean daily temperature of the air was 6.9 °C, registered in May 10th 2016, and the highest mean daily soil temperature was 6.1 °C, recorded in January 30th 2017, at 5 cm soil depth (Figure 2). Between March 2015 and December 2018, there was an increase of the mean annual air and soil temperatures for all soil depths,

although they remained below 0 °C (Table II). At all soil depths, 2015 presented the lower mean annual soil temperatures compared with subsequent years. The 5 cm depth presented the highest mean annual soil temperature for all period, except in 2015, with the lowest one recorded in association with the coldest year, where near surface the active layer is the most influenced by cold air temperatures. On the other hand, the lowest mean annual soil temperature for all the analyzed period was recorded at 50 cm depth. Between 2016 and 2017 the mean annual soil temperatures at all soil depths presented a slight decreasing trend, increasing again from 2017 to 2018. The mean annual SMC increased during the analyzed period, being higher in 2018 at all soil depths (Table II). The 100 cm soil depth presented the highest mean annual SMC in all years, except in 2016, in which the 10 cm depth presented the highest SMC. On the other hand, the 30 cm soil depth presented the lowest SMC in all years, except in 2015, in which the 10 cm depth had the lowest SMC value.

Although daily freeze and thaw cycles were observed during summer, the active layer remained with positive temperatures until, mostly, early April, when the 5 cm soil depth reaches negative temperatures: -0.03 in 2015, -0.06 in 2016, -0.37 in 2017 and -0.02 °C in 2018 (Figure 2). The SMC begins a sharp decrease on April, in 2015 and 2016, and on May, in 2017 and

Table I. Physical and morphological attributes of the soil of Half Moon Island.

Horizon, depth (cm)	CS[a]	FS[b]	Silt[c]	Clay[d]	Class
------------------ g.kg^{-1} --------------------					
A 0-7	0,554	0,266	0,136	0,044	Loamy Fine Sand
B1 7-15	0,415	0,301	0,239	0,045	Sandy Loam
B2 15-25	0,34	0,221	0,337	0,102	Sandy Loam
C 25-100	0,488	0,216	0,208	0,087	Sandy Loam
Cg 100+	0,519	0,254	0,159	0,068	Sandy Loam

[a]Coarse sand (0.2–<2 mm), [b]Fine sand (0.05–<0.2 mm), [c]0.002–<0.05 mm, [d]<0.002 mm.

2018, reaching the lowest records between June and August, and peaking on June 16th 2015 the 10 cm depth (Figure 3). The complete freezing of the active layer along the years occurred after the 100 cm soil depth reaches consistent negative temperature, which occurred on May 20th 2015, April 25th 2016, May 28th 2017 and May 28th 2018. The subsequent cooling resulted in the lower minimum annual soil temperatures for each year during the winter, with 2015 presenting the coldest values at all soil depths (Table II). Along the analyzed period, in general, the minimum annual soil temperatures at all depths increased, indicating consistent warmer conditions in 2018.

The soil temperatures began to rise in September, during spring, but remained negative and close to 0 °C, showing a strong zero curtain effect (Figure 2). The soil presented positive temperatures in January, during summer, when the 5 cm depth reached 0.01 °C. From 2017 to 2018, the 5 cm soil depth reached positive temperature at an earlier date, in December. The complete thawing of the active layer occurred when the 100 cm soil depth reached consistent positive temperatures, which was of 0.01 °C on February 29th 2016, 0.02 °C on January 10th 2017 and 0.03 °C on December 31th 2017. The year 2017 was the only that presented positive temperatures during December, showing a mean daily temperature of 0.46 and 0.09 °C at 5 and 10 cm depths (Table II). Maximum annual soil temperatures were registered in the summer, with the 5 cm depth reaching the highest maximum value of 12.06 °C on January 30th 2017. In 2017, the 5 and 10 cm soil depths presented higher maximum annual temperatures, whereas in 2018, the 30, 50 and 100 cm soil depths presented the higher readings (Table II). Positively mean monthly temperatures at 100 cm soil depth occurred on February and March, in 2015 and 2016, and between February and April in 2017, and from January to April in

2018, showing a wider thawing period variability at the bottommost layer, where permafrost table is present (Table II). The period in which the SMC was higher than 10% increased along years (Figure 3).

During autumn and winter, deeper horizons showed higher temperatures (although negative) than shallow depths, with an opposite behavior during spring and summer (Table II). This is due to the proximity of the soil surface with the atmosphere, being more susceptible to changes than the thermally buffer subsurface soil. According to the histograms (Figure 4), for the first 50 cm soil depth higher frequency was found in the -0.5 and 0 °C range, and at 100 cm depth most reads prevailed between 0 and 0.5 °C.

The additional decomposition of the temperature time series at different depth layers helps to differentiate the thermal behavior within the active layer. At the surface the remainder component of the series varies between -2 and 4 °C, with a seasonal component between -2 and 2 °C, both are concentrated in the summer. At the beginning of the evolution of the freezing front, both showed an increase in volatility, for a longer period for 2017 and 2018 (Figure 5). The trend also shows 2015 as a colder year, with a much longer period of negative temperatures (Figure 5).

Positive temperatures are limited in time, being progressively grater over the analyzed period (Figure 5). In 2015, the surface active layer showed a great resistance in crossing the 0 °C barrier, with persisting temperatures close to the freezing point, indicating a zero curtain effect (Outcalt et al. 1990). The behavior at 10 cm is very similar, while temperature variations in all years are lessened (Figure 5). At 30 cm temperatures vary in a shorter range, the remainder and seasonal components are less expressive and more concentrated in time. In 2015 and 2016,

Table II. Mean monthly temperatures of the air and soil and mean monthly soil moisture content at 5, 10, 30, 50 and 100 cm depth. Annual mean, minimum, maximum and standard deviation calculated from hourly readings of the air and soil temperatures and of the soil moisture content at all depths.

Month	2015									
	Temperature (°C)						Soil moisture content (%)			
	Air	5	10	30	50	100	10	30	50	100
Mar.	0.84	0.19	0.14	0.11	0.02	0.09	37.63	26.25	39.84	39.15
Apr.	0.10	-0.17	-0.04	0.05	-0.01	0.07	18.45	24.26	34.32	35.83
May	-2.24	-2.08	-1.76	-0.78	-0.50	-0.27	5.66	9.90	13.24	16.21
June	-6.29	-5.09	-4.89	-3.95	-3.47	-3.05	4.74	5.80	7.11	8.26
July	-7.56	-4.48	-4.39	-3.93	-3.72	-3.45	4.72	5.73	7.00	8.10
Aug	-6.31	-4.37	-4.30	-3.91	-3.76	-3.53	4.74	5.72	7.00	8.10
Sept.	-7.00	-4.97	-4.90	-4.49	-4.32	-4.09	4.71	5.65	6.95	8.10
Oct.	-1.94	-3.13	-3.16	-3.17	-3.25	-3.17	4.87	5.79	7.00	8.12
Nov.	-1.28	-1.95	-2.00	-2.08	-2.21	-2.15	5.00	5.93	7.11	8.24
Dec.	0.47	-0.15	-0.26	-0.58	-0.84	-0.86	6.12	6.54	7.43	8.56
Mean	-3.11	-2.62	-2.55	-2.27	-2.20	-2.04	9.68	10.15	13.70	14.86
Max.	9.71	2.29	1.71	0.68	0.28	0.21	41.6	36.9	40.5	39.7
Min.	-17.68	-9.08	-8.30	-5.89	-4.84	-4.35	4.6	5.6	6.9	8
SD	4.38	2.12	2.05	1.80	1.67	1.60	10.91	8.16	12.11	11.81
	2016									
Month	Temperature (°C)						Soil moisture content (%)			
	Air	5	10	30	50	100	10	30	50	100
Jan.	0.85	0.06	-0.09	-0.24	-0.41	-0.38	8.61	7.40	8.25	9.21
Feb.	1.10	1.55	1.00	0.18	-0.03	0.00	38.89	24.66	13.47	13.26
Mar.	1.12	0.86	0.73	0.36	0.12	0.08	38.03	26.44	38.19	31.34
Apr.	-2.43	-1.64	-1.23	-0.39	-0.18	-0.03	20.76	17.47	25.13	24.31
May	-0.16	-2.24	-2.17	-1.77	-1.59	-1.37	5.90	5.92	6.77	8.33
June	-1.58	-1.52	-1.51	-1.42	-1.47	-1.36	6.04	6.00	6.75	8.29
July	-4.22	-2.76	-2.68	-2.28	-2.12	-1.92	5.73	5.84	6.64	8.17
Aug	-6.20	-3.30	-3.24	-2.88	-2.73	-2.53	5.64	5.71	6.52	8.05
Sept.	-1.02	-1.07	-1.18	-1.43	-1.63	-1.64	6.14	6.00	6.63	8.13
Oct.	-0.82	-0.16	-0.23	-0.41	-0.61	-0.60	6.90	6.50	6.98	8.48
Nov.	-0.36	-0.09	-0.14	-0.26	-0.42	-0.40	7.28	6.79	7.13	8.69
Dec.	0.69	-0.02	-0.07	-0.17	-0.33	-0.29	8.04	7.08	7.30	8.87
Mean	-1.10	-0.87	-0.91	-0.90	-0.96	-0.88	13.06	10.42	11.64	12.09
Max.	12.81	9.20	5.96	1.18	0.42	0.14	40.2	32.2	38.9	35.1
Min.	-17.93	-7.41	-5.92	-3.57	-3.34	-3.10	5.3	5.6	6.4	7.9
SD	3.37	1.84	1.59	1.13	0.97	0.89	12.75	7.97	10.30	7.96
	2017									
Month	Temperature (°C)						Soil moisture content (%)			
	Air	5	10	30	50	100	10	30	50	100

Table II. Continuation.

Month	Air	5	10	30	50	100	10	30	50	100
Jan.	1.39	1.78	1.23	0.37	0.05	-0.01	24.18	18.62	20.48	15.83
Feb.	1.75	2.84	2.53	1.57	0.96	0.73	35.38	23.38	33.25	36.76
Mar.	1.46	1.44	1.24	0.82	0.54	0.49	34.17	22.13	29.57	35.00
Apr.	-1.08	-0.50	-0.20	0.20	0.11	0.17	24.32	19.64	25.04	31.22
May	-1.69	-1.42	-1.20	-0.47	-0.22	-0.01	6.02	7.99	13.21	16.05
June	-4.68	-3.56	-3.31	-2.41	-2.11	-1.70	5.31	6.70	8.43	7.38
July	-3.89	-2.36	-2.30	-2.03	-2.00	-1.83	5.39	6.58	8.20	7.01
Aug	-5.17	-3.00	-2.94	-2.63	-2.51	-2.34	5.34	6.53	8.13	6.97
Sept.	-4.17	-3.06	-3.04	-2.84	-2.81	-2.66	5.34	6.49	8.09	6.90
Oct.	-2.78	-2.39	-2.40	-2.31	-2.34	-2.24	5.40	6.52	8.10	6.96
Nov.	-0.46	-0.64	-0.75	-0.96	-1.14	-1.13	6.18	6.98	8.39	7.20
Dec.	0.65	0.46	0.09	-0.24	-0.40	-0.35	13.39	7.75	8.84	8.18
Mean	-1.57	-0.89	-0.94	-0.93	-1.00	-0.92	14.07	11.53	14.85	15.31
Max.	5.78	12.06	8.20	2.53	1.45	1.09	39.1	34.5	37.5	38.6
Min.	-16.82	-8.31	-7.60	-5.30	-4.43	-3.72	5	6.3	7.4	6.8
SD	3.83	2.44	2.12	1.54	1.33	1.22	13.02	7.19	9.63	11.63
2018										
Month	**Temperature (°C)**						**Soil moisture content (%)**			
	Air	5	10	30	50	100	10	30	50	100
Jan.	1.48	2.83	2.31	1.01	0.46	0.33	36.80	24.88	29.99	29.57
Feb.	2.47	3.32	3.00	2.07	1.50	1.24	35.05	22.84	30.66	35.03
Mar.	0.68	0.95	0.87	0.70	0.54	0.53	33.88	22.04	27.49	32.80
Apr.	-0.48	0.07	0.12	0.18	0.11	0.17	31.53	20.93	26.03	31.64
May	-1.92	-1.97	-1.46	-0.39	-0.16	0.03	9.30	13.41	19.03	24.86
June	-3.65	-1.22	-1.13	-0.67	-0.51	-0.27	6.28	7.27	9.73	10.27
July	-3.39	-1.48	-1.42	-1.09	-1.03	-0.86	6.07	6.99	9.15	9.24
Aug	-4.55	-1.51	-1.46	-1.22	-1.22	-1.10	6.03	6.96	9.09	9.07
Sept.	-3.48	-1.37	-1.35	-1.20	-1.24	-1.14	6.05	6.95	9.07	9.01
Oct.	-1.63	-1.31	-1.32	-1.24	-1.30	-1.21	6.08	6.94	9.07	9.00
Nov.	-0.24	-0.15	-0.23	-0.36	-0.51	-0.47	7.56	7.56	9.37	9.39
Dec.	0.31	-0.07	-0.13	-0.20	-0.32	-0.27	8.27	7.94	9.60	9.64
Mean	-1.31	-0.19	-0.21	-0.22	-0.32	-0.26	16.40	13.12	16.84	18.69
Max.	8.24	10.4	7.11	3.17	2.27	1.81	38.5	33.6	38.4	38.1
Min.	-14.45	-6.15	-4.75	-1.75	-1.47	-1.32	5.5	6.8	9	9
SD	3.45	2.01	1.70	1.08	0.88	0.76	13.35	7.67	9.74	11.20

positive temperatures are lower than those 2017 and 2018 (Figure 5). At the bottommost layers (50 and 100 cm) the remainder and seasonal components are negligible in 2015 and 2016, whereas the freezing conditions in 2015 are stronger and last longer. Hourly temperature data is equivalent to the trend, and positive temperatures prevail in 2017 and 2018, as evidenced by the variations at remainder and at seasonal components (Figure 5). Considering

daily averages, the ALT reached its maximum of 135.9 cm in late March 2015, 118.4 cm in early March 2016, 168.4 cm in early February 2017 and 242.36 cm at early February 2018.

Freezing regime

Thawing days were concentrated between January and March, occurring at all soil depths except at 50 and 100 cm in 2015 and 2016, which did not present thawing days (Figure 6a). The sum of thawing days during the analyzed period was 215 at 5 cm, 202 at 10 cm, 159 at 30 cm, 117 at 50 cm and 109 at 100 cm depth. The years of 2017 and 2018 presented the highest numbers of thawing days, reaching 86 days at 5 cm depth and 82 days at 10 cm, respectively, and with the lower layers (> 50 cm) presenting the lowest numbers (Figure 6a). On the other hand, freezing days were more frequent than thawing days

and they occurred mainly between May and November at all soil depths (Figure 6b). The sum of freezing days during the entire period was 720 at 5 cm, 725 at 10 cm and at 30 cm, 775 at 50 cm and 739 at 100 cm depth. The years of 2015 and 2016 presented the highest number of freezing days reaching 226 and 201 days at 50 cm depth, respectively, and 2018 presented the lowest number, 139 days at 100 cm soil depth (Figure 6b). The freezing days occurred more frequently at 50 cm soil depth in all years, except in 2018, when it was more frequent at 5 cm depth.

Isothermal days was less frequent during winter at all soil depths and, in general, increased with depth (Figure 6c). The highest values of isothermal days occurred in 2016, reaching a maximum of 180 days at 30 cm soil depth (Figure 6c). Freezing-thawing cycles predominate during December to February and occurred more
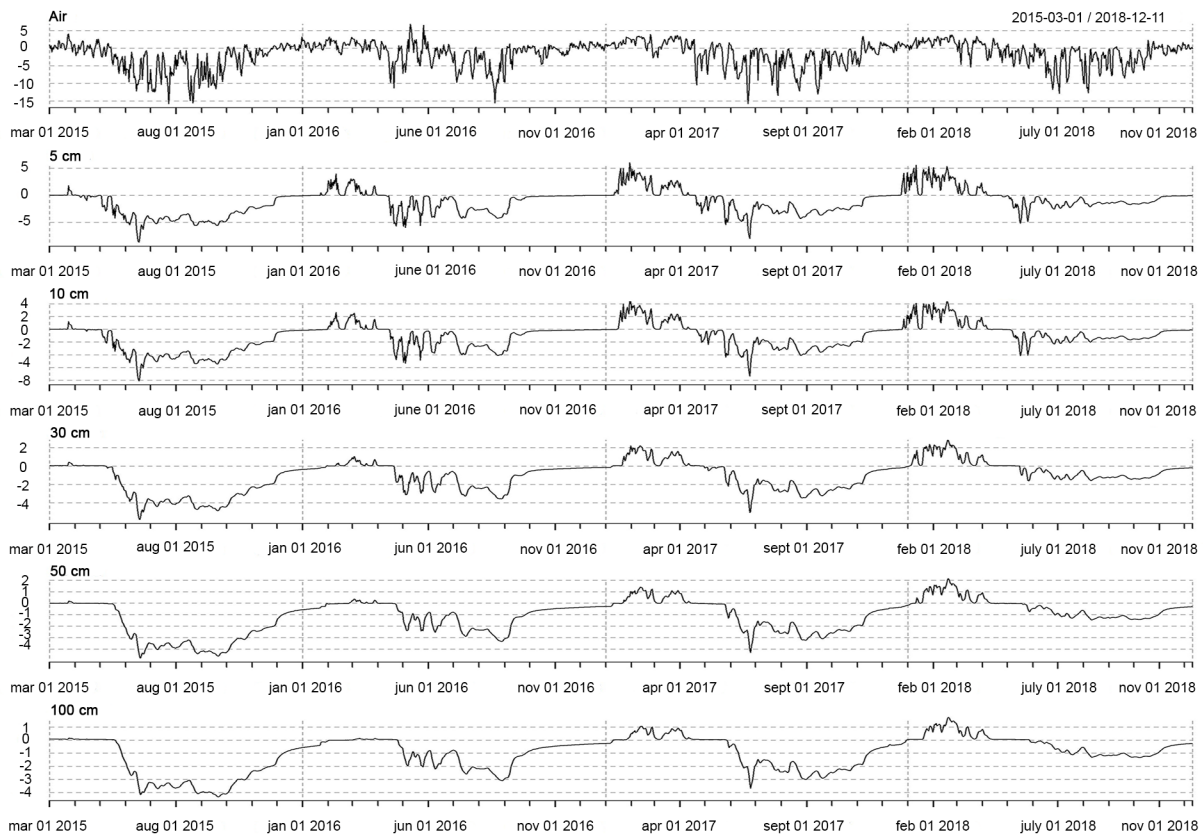
Figure 2. Mean daily temperatures of the air and soil at 5, 10, 30, 50 and 100 cm depths in Half Moon Island.

frequently in December 2018 at all soil depths (Figure 6d). In February 2016, freezing-thawing cycles reached the highest value at 10 cm soil depth (Figure 6d).

The sum of all positive daily temperature averages was not expressive at all depths in 2015, and increased considerably in the following years (Figure 7a). The sum during the study period was 494 °C days at surface, 401.1 °C days at 10 cm, 227.8 °C days at 30 cm, 133.4 °C days at 50 cm and 121 °C days at 100 cm. The cumulative TDD are concentrated between January and March and showed great differences between years, varying from a maximum of 6 °C days at 5 cm depth in 2015 to 213.9 °C days at the same depth in 2018 (Figure 7a). The cumulative FDD were much greater than the TDD, and concentrated between April and December (Figure 7b). The sum of the cumulative FDD during the analyzed period was -2001 at 5 cm, -1929.4 at 10 cm, -1663.9 at 30 cm, -1631.9 cm and 1488.9 °C days at 100 cm depth. In 2015 the cumulative FDD reached the lowest number of -806.3 °C days at 5 cm soil depth and in 2018 it was the highest (-278.8 °C days) at the same depth (Figure 7). The greater values of FFD compared to those of TDD indicate predominate freezing conditions.

DISCUSSION

The soil thermal regime at the small HMI is periglacial although temperature fluctuation bellow 30 cm are limited, with much greater temperature variations near the surface. Minimum temperature at the bottom of the active layer is -4.3 °C; permafrost is typically ice cemented and temperatures are close to freezing point, corroborating with the classification of
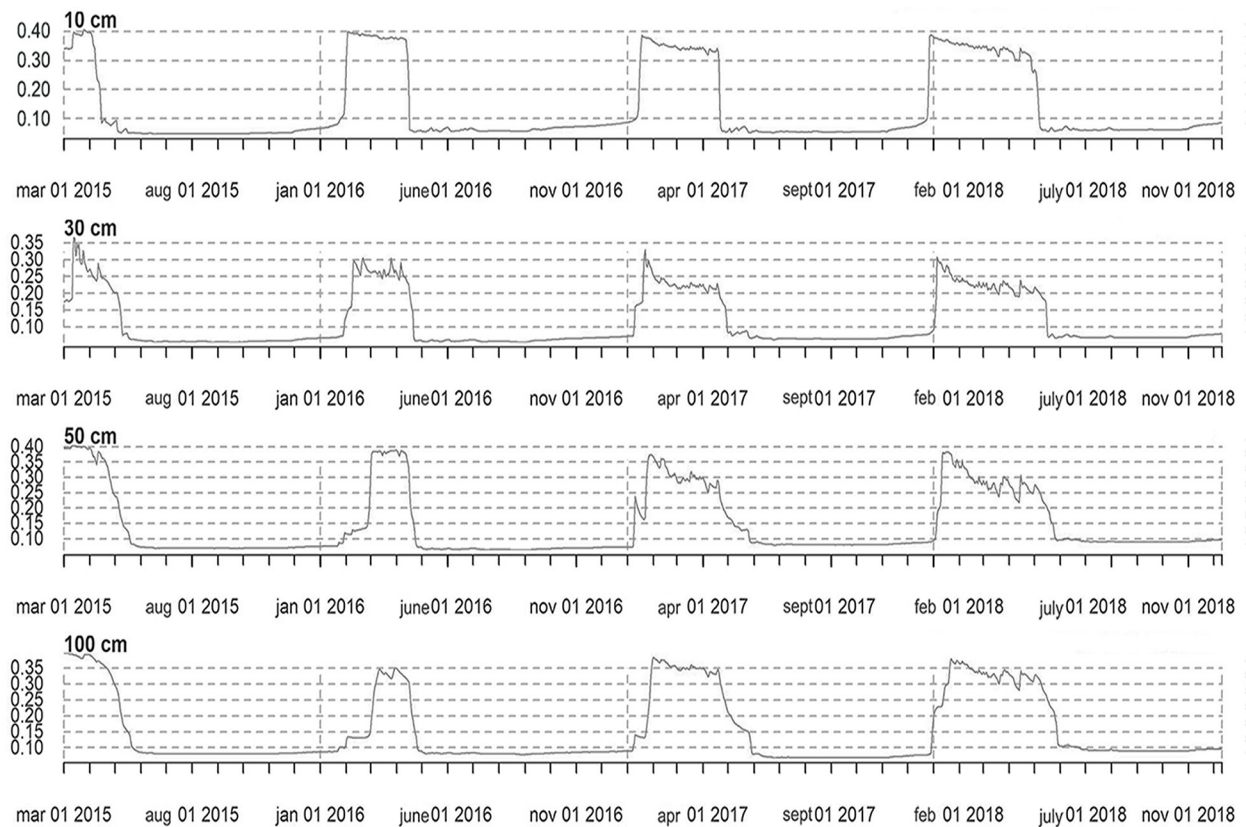
Figure 3. Measurements of the mean daily soil moisture (%) at 10, 30, 50 and 100 cm depths.
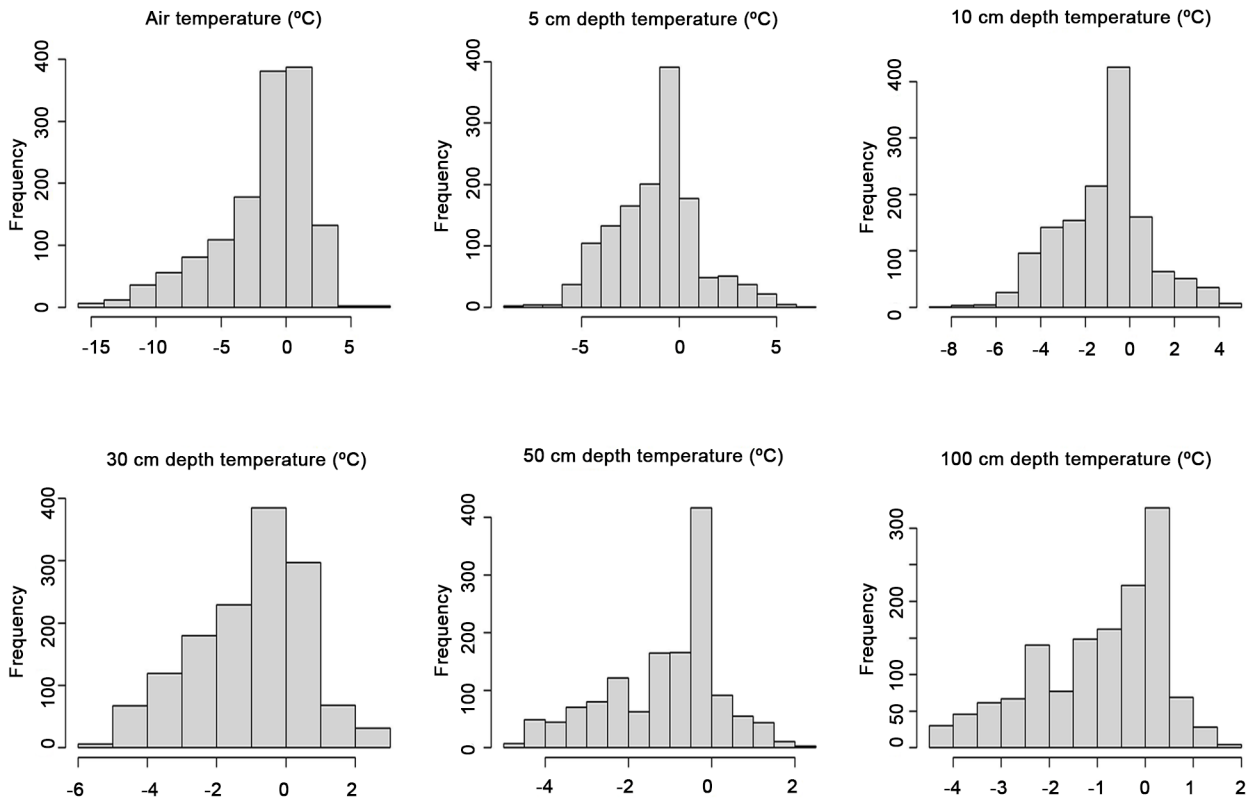
Figure 4. Histograms of the mean daily temperatures of the air and soil at 5, 10, 30, 50 and 100 cm depth.

this soil as Cryosol. Active layer thickness varied between the studied years, reaching a maximum depth in 2018, but as early as 2015 the Argentinian Station water supply was compromised.

Patterned ground occurs at the studied site, but the process appears to be little active in current times, since plant colonization is abundant. These conditions, together with the limited number of freezing–thawing days suggest that permafrost at the tombolo landform might no longer be in equilibrium with the current landscape. The intense Late Holocene uplift experienced by the island (16.8 m) and limited period in which it took place (2.8 mm of uplift per year, 6,000 yr BP) (Fretwell et al. 2010) created conditions for permafrost melting leading to more intense and diverse morphodynamic processes (López-Martínez et al. 2012).

The soil is located at a snow-covered landscape, which influences soil temperatures at surface, and permafrost stability. Air temperature data must be interpreted with care due to the possibility of intense snow cover. Extended periods of snow cover on the soil surface, reduces the heat exchange between soil and atmosphere, and affects the energy balance of the surface, buffering changes in soil temperature for a longer period (Schaefer et al. 2017b). This confirms that the snow cover is an important factor controlling the air-ground interface, similar results were found in several sites in the Antarctic continent (Vieira et al. 2010), in the Eastern Antarctic Peninsula (Hrbáček et al. 2015, 2016, Schaefer et al. 2017b) and in the Maritime Antarctica, mostly in the SSI, such as in Byers Peninsula (de Pablo et al. 2017, Oliva et al. 2016), Deception Island (Goyanes et al. 2014), Livingston Island (Ferreira et al. 2017), and Keller and Fildes Peninsula at King George
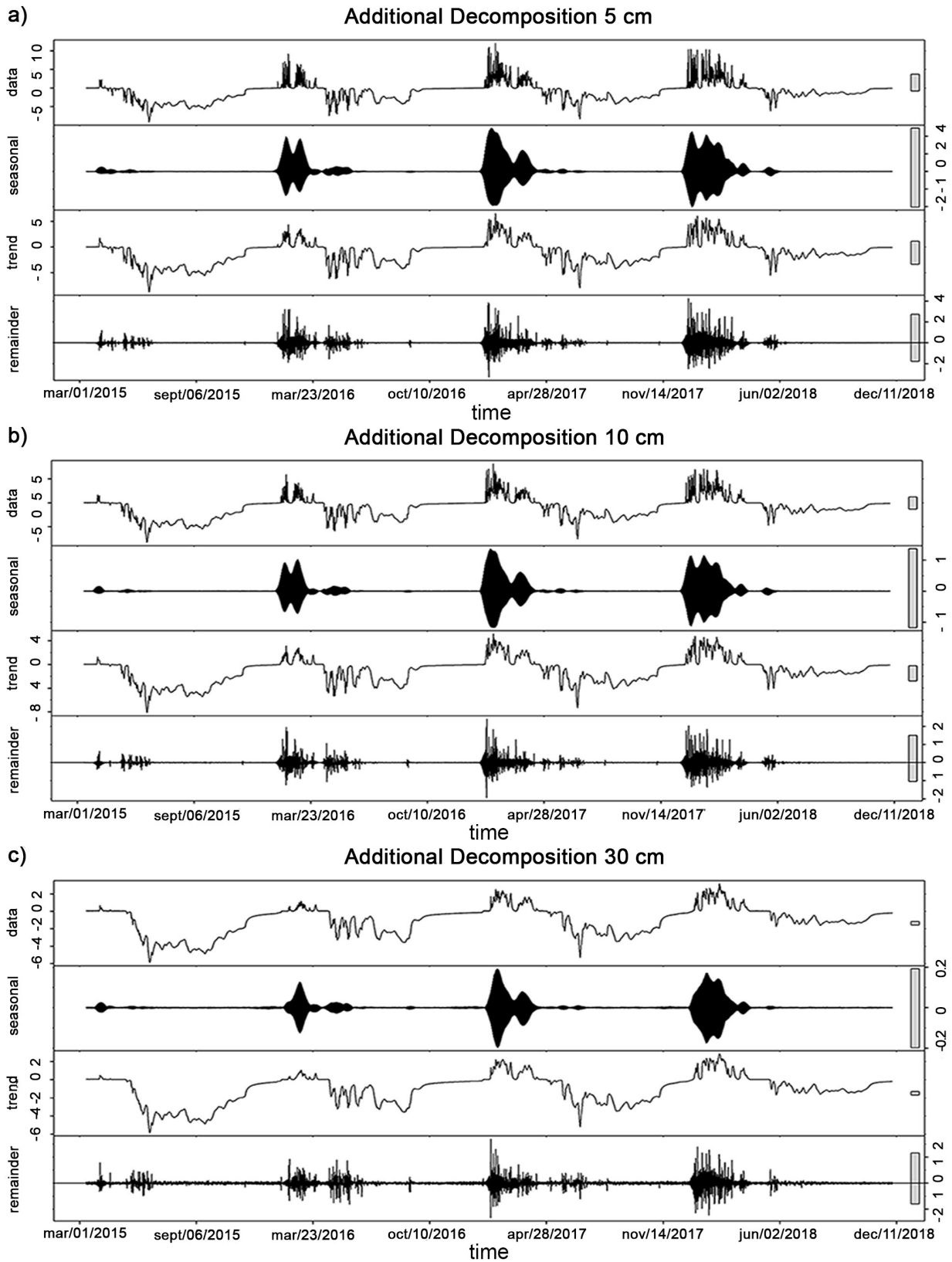
Figure 5. Additional decomposition of the daily time series at 5 (a), 10 (b) and 30 (c) cm depth.
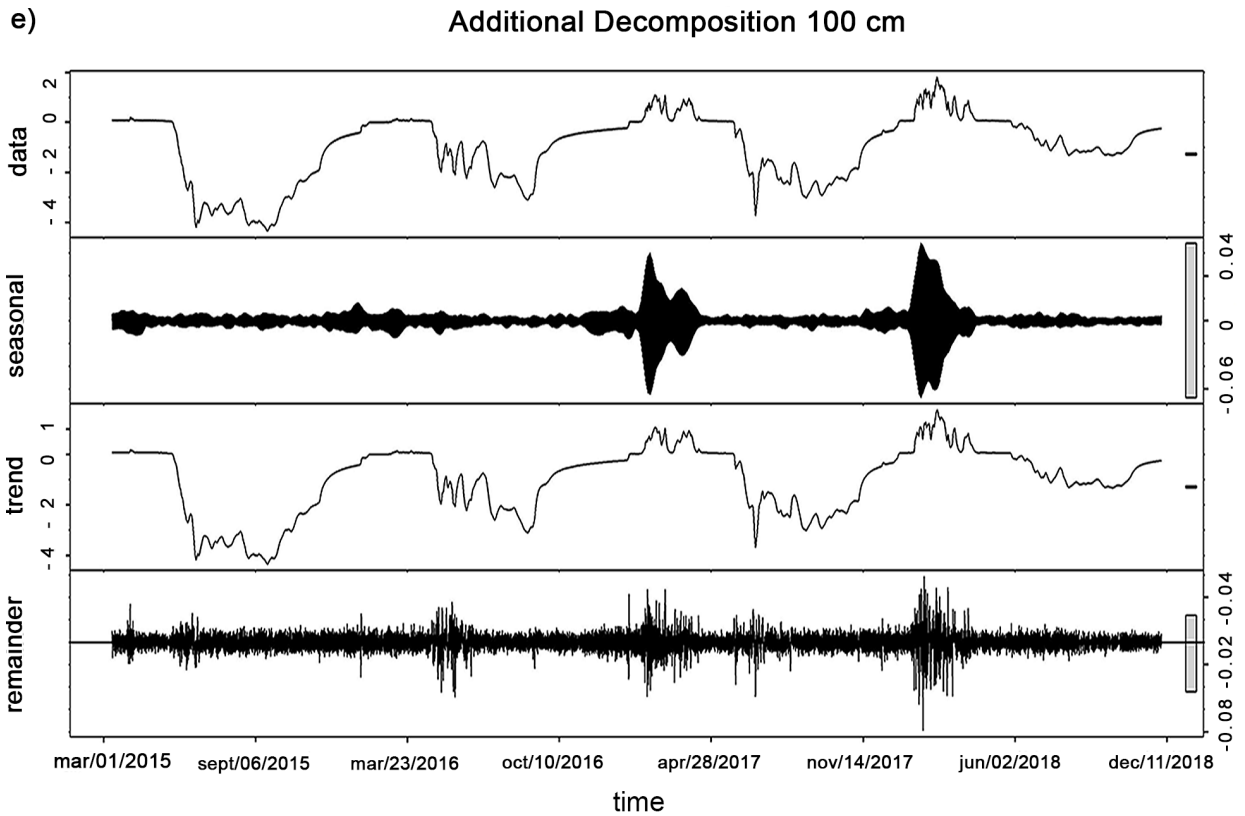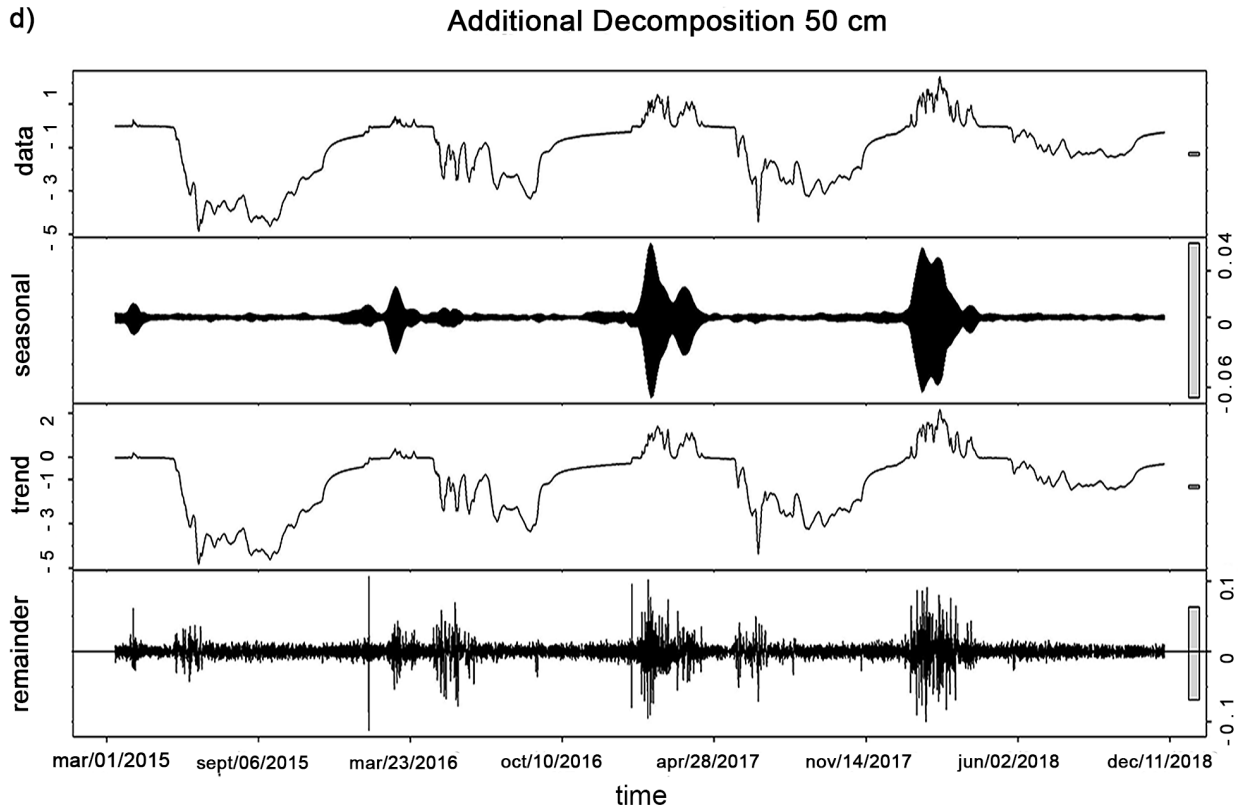
Figure 5. (Continued) Additional decomposition of the daily time series at 50 (d) and 100 (e) cm depth.

Island (Chaves et al. 2017, Michel et al. 2014, respectively).

The soil has a textural change at 25 cm, to a coarser one, with increasing gravel content, resulting from the marine sedimentation. The water soil content was high during the thawing period, due to the snow pack melting, and experienced little variations with depth, due to good internal drainage, promoting a buffered effect on temperature variations, near 0 °C. This situation is the classical zero curtain effect, already observed in similar periglacial sites in the Maritime Antarctica (Almeida et al. 2017, Michel et al. 2014, Schaefer et al. 2017b). SMC remains high through the soil and the thawing season increased over the years, being greater in 2018. ALT at HMI shows high variability between the years, with 2015 as a colder year, when maximum temperature at the bottom of the profile and the thermal gradient in relation to the 50 cm layer were considerable.

The decomposition of the time series illustrates how the time series are stationary in its essence. Noise is increasing over the years; the trend component over the thaw period is also more pronounced as time goes by and is present for a longer period. All fluctuations are attenuated with depth although the seasonal component is neglectable in 2015 at 100 cm, indicating preservation of the frozen layer. The trend component highlights the time it takes to break the freezing point in the thaw season, the texture of the profile reduces water retention and limits the zero curtain effect (temperature buffering near the freezing point), while the study period shows greater resistance in the freezing point in the thaw season of 2016.
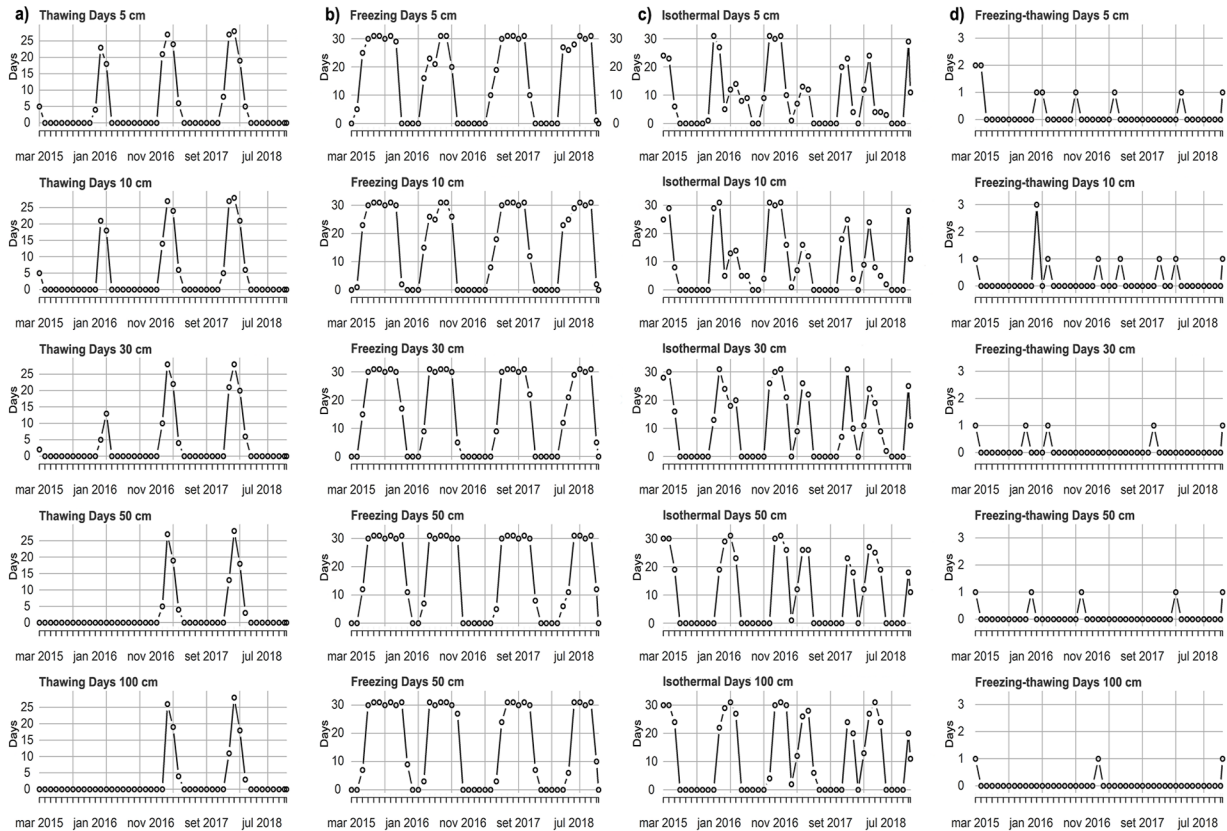
Figure 6. Thawing days (a), freezing days (b), isothermal days (c) and freezing-thawing cycles (d) during 2015 – 2018 at 5, 10, 30, 50 and 100 cm soil depth.

While the seasonal period in which the bottommost layer remains unfrozen is short, the landscape effects are evident, since permafrost melting promote great hydrological implications, with sudden changes in adjacent lakes and pools (Bockheim et al. 2013). The uplifted marine terrace where the monitoring system was installed is exposed to both sides of the coast, making it more vulnerable to geomorphic disturbances. Also, we should consider the fact that all man-made structures of the island were built over this fossil beach (Figure 1). Climate change in the Shetland Islands increases permafrost degradation leading to greater geomorphic dynamics and slope erosion from the upper platforms to the coast line (Cannone et al. 2006, Vieira et al. 2008).

Although uplifted marine terraces are considered stable low entropy environments, the presence of permafrost associated with poor drainage, resulting in water saturation during thawing period, affects the thermal regime and implies very dynamic processes in the active layer (López-Martínez et al. 2016). Permafrost degradation at HMI not only alter soil drainage, but also triggers further lowering of the permafrost table. Hence, uplifted marine terraces offer a suitable environment for periglacial morphodynamics systems with intense sediment transfer and slope processes (Bockheim et al. 2013). The increasing intensity of periglacial morphodynamics at the Holocene uplifted terraces is yet to be investigated given its ecological importance for vegetation growth.
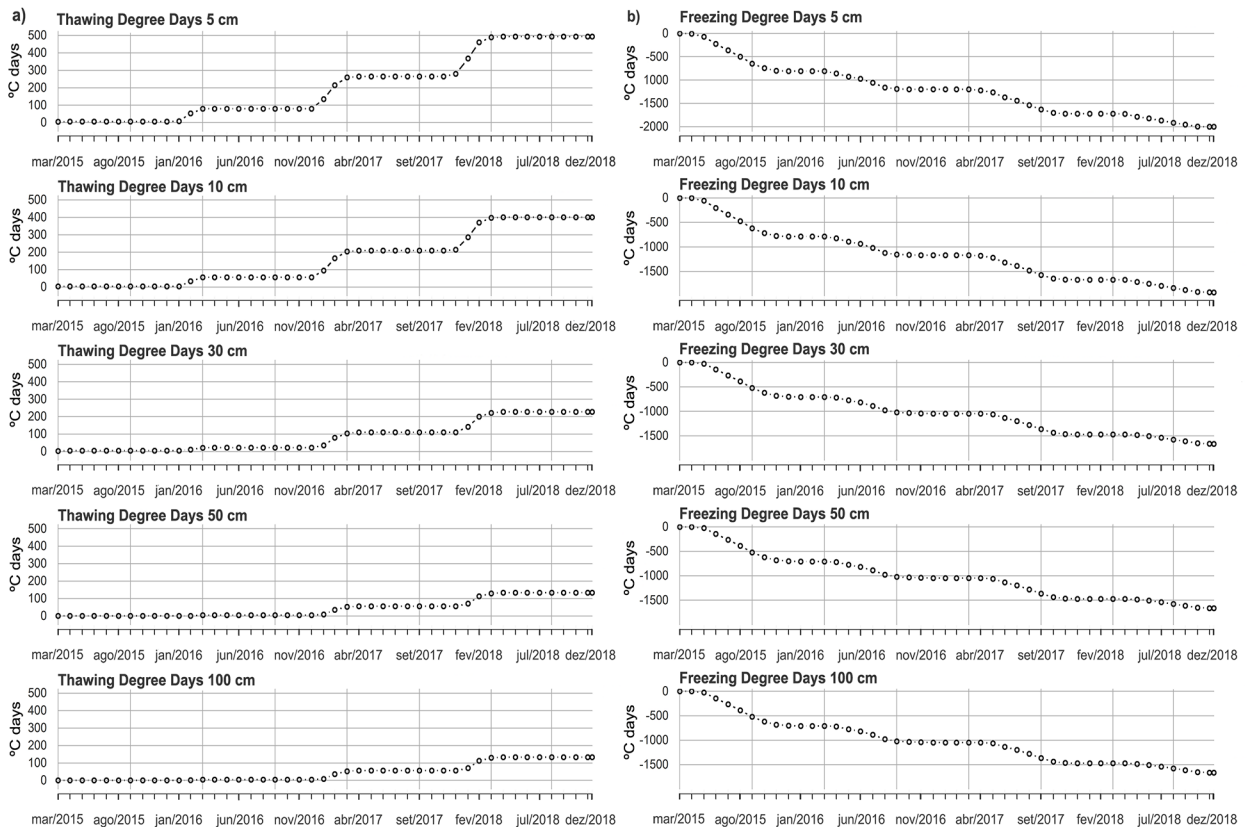
Figure 7. Thawing degree days (a) and freezing degree days (b) during 2015 – 2018 at 5, 10, 30, 50 and 100 cm soil depth.

CONCLUSIONS

1) The active layer thermal regime of a low-lying Cryosol at Half Moon Island, over a four-year period, shows a dominance of freezing conditions, with active layer thickness reaching a maximum of 242 cm during late March 2018, as a response of air temperature variations.

2) These large variations in the active layer depth highlight the strong intrinsic interannual variability of the local permafrost, reaching deeper layers over the analyzed period, highlighting a degradation trend

3) The intense late Holocene uplift of marine terraces experienced by HMI, counteracted with recent air temperature variations, affect the active layer depth and drainage properties of the unusual, relict patterned ground, where Cryosols are found, on the upper marine terrace. Longer monitoring periods are necessary for a detailed understanding on how current climatic and geomorphic conditions affect permafrost and the morphodynamics of HMI, in relation to other uplifted marine terraces spread over the SSI.

Acknowledgments

REFERENCES

ALMEIDA ICC, SCHAEFER CEGR, FERNANDES RBA, PEREIRA TTC, NIEUWENDAM A & PEREIRA AB. 2014. Active layer thermal regime at different vegetation covers at Lions Rump, King George Island, Maritime Antarctica. Geomorp 225: 36- 46.

ALMEIDA ICC, SCHAEFER CEGR, MICHEL RFM, FERNANDES RBA, PEREIRA TTC, ANDRADE AM, FRANCELINO, MR, FERNANDES FILHO EI & BOCKHEIM JG. 2017. Long term active layer monitoring at a warm-based glacier front from Maritime Antarctica. Catena 149: 572-581.

ARAYA R & HERVÉ F. 1972. Patterned gravel beaches in South Shetland. In: Adie RJ (Ed), Antarctic Geology and Geophysics: International Union of Geological Science, Oslo Series B, p. 111-114.

BOCKHEIM JG. 1995. Permafrost distribution in the southern circumpolar region and its relation to the environment: A review and recommendations for further research. Permafrost Perigl Process 6: 27-45.

BOCKHEIM JG, RAMOS M, LÓPEZ-MARTÍNEZ J, SERRANO E, GUGLIELMIN M, WILHELM K & NIEUWENDAM A. 2013. Climate warming and permafrost dynamics in the Antarctic Peninsula region. Global Planet Chang 100: 215-223.

BOCKHEIM JG & TARNOCAI C. 1998. Nature, occurrence and origin of dry permafrost. In: Lewkowicz AG & Allard M (Eds), Proc. Seventh International Conference on Permafrost. Collection Nordica (Université Laval) 57, p. 57-64.

CANNONE N, ELLIS-EVANS JC, STRACHAN R & GUGLIELMIN M. 2006. Interactions between climate, vegetation and the active layer in soils at two Maritime Antarctic sites. Antarctic Science 18: 323-333.

CHAVES D, LYRA G, FRANCELINO M, SILVA L, THOMAZINI A & SCHAEFER CEGR. 2017. Active layer and permafrost thermal regime in a patterned ground soil in Maritime Antarctica, and relationship with climate variability models. Sci of The Total Environ 584-585: 572-585.

CLEVELAND RB, CLEVELAND WS, MCRAE JE & TERPENNING I. 1990. STL: A Seasonal-Trend Decomposition Procedure Based on Loess. J Off Stat 6: 3-73.

CURL JE. 1980. A Glacial History of the South Shetland Islands, Antarctica. Institute of Polar Studies Report No. 63, Institute of Polar Studies, The Ohio State University, 129 p.

DE PABLO MA, BLANCO JJ, MOLINA A, RAMOS M, QUESADA A & VIEIRA, G. 2013. Interannual active layer variability at the Limnopolar Lake CALM site on Byers Peninsula, Livingston Island, Antarctica. Antarc Scien 25(2): 167-180.

DE PABLO MA, RAMOS M & MOLINA A. 2014. Thermal characterization of the active layer at the Limnopolar Lake CALM-S site on Byers Peninsula (Livingston Island), Antarctica. Solid Earth, 5: 721-739.

DE PABLO MA, RAMOS M & MOLINA A. 2017. Snow cover evolution, on 2009-2014, at the Limnopolar Lake CALM-S site on Byers Peninsula, Livingston Island, Antarctica., Catena 149: 538-547.

DOBIŃSKI W. 2020. Permafrost active layer. Earth-Science Reviews 208(103301).

FERREIRA A, VIEIRA G, RAMOS M & NIEUWENDAM A. 2017. Ground temperature and permafrost distribution in Hurd Peninsula (Livingston Island, Maritime Antarctic): An assessment using freezing indexes and TTOP modelling. Catena 149: 560-571.

FRANCELINO MR, SCHAEFER CEGR, SIMAS FNB, FERNANDES FILHO EI, SOUZA JJLL DE & COSTA LM DA. 2011. Geomorphology and soils distribution under paraglacial conditions in an ice-free area of Admiralty Bay, King George Island, Antarctica. Catena 85: 194-204.

FRETWELL PT, HODGSON DA, WATCHAM EP, BENTLEY MJ & ROBERTS SJ. 2010. Holocene isostatic uplift of the South Shetland Islands, Antarctic Peninsula, modelled from raised beaches. Quaternary Science Reviews 29: 1880-1893.

GEE GW & BAUDER JW. 1986. Particle-size analysis. in: Methods of Soil Analysis, Part 1: Physical and Mineralogical Methods. Klute A (Ed). Soil Science Society of America, Madison, Wisconsin: 383-412.

GOYANES G, VIEIRA G, CASELLI A, CARDOSO M, MARMY A, SANTOS F, BERNARDO I & HAUCK C. 2014. Local influences of geothermal anomalies on permafrost distribution in an active volcanic island (Deception Island, Antarctica). Geomorp 225: 57-68.

GUGLIELMIN M. 2006. Ground surface temperature (GST), active layer and permafrost monitoring in continental Antarctica. Permafrost Perigl Process17: 133-143.

GUGLIELMIN M & CANNONE N. 2012. A permafrost warming in a cooling Antarctica? Climatic Change 111: 177-195.

GUGLIELMIN M, DALLE FRATTE M & CANNONE N. 2014. Permafrost warming and vegetation changes in continental Antarctica. Environmental Research Letters, 9. doi:10.1088/1748-9326/ 9/4/045001

GUGLIELMIN M, ELLIS EVANS CJ & CANNONE N. 2008. Active layer thermal regime under different vegetation conditions in permafrost areas. A case study at Signy Island (Maritime Antarctica). Geoder 144: 73-85.

GUGLIELMIN M, WORLAND MR & CANNONE N. 2012. Spatial and temporal variability of ground surface temperature and active layer thickness at the margin of maritime Antarctica, Signy Island. Geomorp 155: 20-33.

HRBÁČEK F ET AL. 2018. Active layer monitoring in Antarctica: an overview of results from 2006 to 2015. Pol Geogr 1-16.

HRBÁČEK F, CANNONE N, KŇAŽKOVÁ M, MALFASI F, CONVEY P & GUGLIELMIN M. 2020. Effect of climate and moss vegetation on ground surface temperature and the active layer among different biogeographical regions in Antarctica. Catena 190: 104562.

HRBÁČEK F, LÁSKA K & ENGEL Z. 2015. Effect of Snow Cover on the Active-Layer Thermal Regime - A Case Study from James Ross Island, Antarctic Peninsula. Permafrost Perigl Process 27(3): 307-315.

HRBÁČEK F, NÝVLT D & LÁSK A K. 2016. Active layer thermal dynamics at two lithologically different sites on James Ross Island, Eastern Antarctic Peninsula. Catena 149: 592-602.

ISSS WORKING GROUP RB. 1988. World Reference Base for Soil Resources. International Society of Soil Sciences (ISSS). International Soil Reference and Information Centre (ISRIC) and Food and Agriculture Organization of the United Nations (FAO). World Soil Report 84. FAO, Rome, 128 p.

LÓPEZ-MARTÍNEZ J, SCHMID T, SERRANO E, MINK S, NIETO A & GUILLASO S. 2016. Geomorphology and landforms distribution in selected ice-free areas in the South Shetland Islands, Antarctic Northern Peninsula region. Cuad de Inves Geogr 42(2): 35-455.

LÓPEZ-MARTÍNEZ J, SERRANO E, SCHMID T, MINK S & LINÉ SC. 2012. Periglacial processes and landforms in the South Shetland Islands (northern Antarctic Peninsula region). Geomorp 155-156: 62-79.

MARTINEZ GA & MASSONE HE. 1995. Geomorfología de la Isla Media Luna, Islas Shetland del Sur, Antártida. Thalassas 11: 9-26.

MICHEL RFM, SCHAEFER CEGR, POELKING EL, SIMAS FNB, FERNANDES FILHO EI & BOCKHEIM JG. 2012. Active layer temperature in two Cryosols from King George Island, Maritime Antarctica. Geomorp 155-156: 12-19.

MICHEL RFM, SCHAEFER CEGR, SIMAS FMB, FRANCELINO MR, FERNANDES-FILHO EI, LYRA GB & BOCKHEIM JG. 2014 Active-layer thermal monitoring on the Fildes Peninsula, King George Island, Maritime Antarctica. Solid Earth 5: 1361-1374.

OLIVA M. 2016. The deglaciation of the ice-free areas in the South Shetland Islands: examples from Byers (Livingston) and Barton (King George). Cuaternario y Geomorfologia, 30(1-2): 105-118.

OLIVA M, NAVARRO F, HRBÁČEK F, HERNÁNDEZ A, NÝVLT D PEREIRA P & TRIGO R. 2017. Recent regional climate cooling

on the Antarctic Peninsula and associated impacts on the cryosphere. Sci Tot Environ 580: 210-223.

OUTCALT SI, NELSON FE & HINKEL KM. 1990. The zero-curtain effect: heat and mass transfer across an isothermal region in freezing soil. Water Resourc Resear 26: 1509-1516.

RAMOS M, VIEIRA G, DE PABLO MA, MOLINA A, ABRAMOV A & GOYANES G. 2017. Recent shallowing of the thaw depth at Crater Lake, Deception Island, Antarctica (2006–2014). Catena 149: 519-528.

RAMOS M, VIEIRA G, DE PABLO MA, MOLINA A & JIMENEZ JJ. 2020. Transition from a Subaerial to a Subnival Permafrost Temperature Regime Following Increased Snow Cover (Livingston Island, Maritime Antarctic). Atmosphere 11: 1332.

R CORE TEAM. 2020. R: A language and environment for statistical computing. R Foundation for Statistical Computing, Vienna, Austria.

SCHAEFER CEGR, MICHEL RFM, DELPUPO C, SENRA EO, BREMER UF & BOCKHEIM JG. 2017a. Active layer thermal monitoring of a Dry Valley of the Ellsworth Mountains, Continental Antarctica. Catena 149: 603-315.

SCHAEFER CEGR, PEREIRA TTC, ALMEIDA ICC, MICHEL RFM, CORRÊA GR, FIGUEIREDO LPS & KER JC. 2017b. Penguin activity modify the thermal regime of active layer in Antarctica: A case study from Hope Bay. Catena 149: 582-591.

SCHMITZ D, PUTZKE J, ALBUQUERQUE MP, SCHÜNEMANN AL, VIEIRA FCB, VICTORIA FC & PEREIRA AB. 2018. Description of plant communities on Half Moon Island, Antarctica. Polar Research 37: 1-2.

SERRANO E & LÓPEZ-MARTÍNEZ J. 1997. Evolución de las formas de relieve y los depósitos superficiales cuaternarios en la Isla Media Luna. Islas Shetland del Sur. Boletín Real Sociedad Española de Historia Natural 93: 207-218.

SILVA TH, SILVA DAS, OLIVEIRA FS, SCHAEFER CEGR, ROSA CA & ROSA LH. 2020. Diversity, distribution, and ecology of viable fungi in permafrost and active layer of Maritime Antarctica. Extremophiles. doi:10.1007/s00792-020-01176-y.

SMELLIE JL, PANKHURST RJ, THOMSON MRA & DAVIES RES. 1984. The geology of the South Shetland Islands: VI. stratigraphy, geochemistry and evolution. Brit Antar Surv Scient Rep 87: 1-85.

SMITH MW. 1990. Potential responses of permafrost to climatic change. Jour of Cold Regi Engine 41: 29-37.

TURNER J ET AL. 2005. Antarctic climate change during last 50 years. Int J Climatol 25: 279-294.

TURNER J ET AL. 2016. Absence of 21st century warming on Antarctic Peninsula consistent with natural variability. Nature 535: 411-415.

VIEIRA G, LÓPEZ-MARTÍNEZ J, SERRANO E, RAMOS M, GRUBER S, HAUCK C & BLANCO JJ. 2008. Geomorphological observations of permafrost and ground-ice degradation on Deception and Livingston Islands, Maritime Antarctica. Proceedings of the 9th International Conference on Permafrost 2008, p. 1839-1844.

VIEIRA G ET AL. 2010. Thermal state of permafrost and active-layer monitoring in the Antarctic: advances during the international polar year 2007–2009. Permafrost Perigl Process 21:182-197.

WILHELM KR & BOCKHEIM JG. 2016. Climatic controls on active layer dynamics: Amsler Island, Antarctica. Antarc Scien 29(02): 173-182.

CARLOS ERNESTO G.R. SCHAEFER[1]
https://orcid.org/0000-0001-7060-1598

MÁRCIO R. FRANCELINO[1]
https://orcid.org/0000-0001-8837-1372

ANTONIO B. PEREIRA[2]
https://orcid.org/0000-0003-0368-4594

ROBERTO F.M. MICHEL[3]
https://orcid.org/0000-0001-5951-4610

DANIELA SCHMITZ[1]
https://orcid.org/0000-0002-3162-2430

IORRANA F. SACRAMENTO[1]
https://orcid.org/0000-0002-9440-0034

WILLIAM F. RODRIGUES[4]
https://orcid.org/0000-0003-0980-282X

CAIK O. DE MIRANDA[1]
https://orcid.org/0000-0002-3510-2678

[1]Federal University of Viçosa, PH Rolfs Avenue, s/n, Department of Soil, Center, 36570-000 Viçosa, MG, Brazil

[2]Federal University of Pampa, Antônio Trilha Avenue, 1847, Vila Camita, 97300-162 São Gabriel, RS, Brazil

[3]Federal University of Santa Cruz, Jorge Amado Road, Km 16, Department of Agrarian and Environmental Sciences, Salobrinho, 45662-900 Ilhéus, BA, Brazil

[4]Federal University of Ouro Preto, Diogo de Vasconcelos Street, 122, Department of Geology, Pilar, 35402-163, Ouro Preto, Minas Gerais, Brazil

Correspondence to: **Iorrana Figueiredo Sacramento**
E-mail: iorrana.figueiredo@ufv.br

Author contributions

The authors Carlos E.G.R. Schaefer, Márcio R. Francelino and Antonio Batista Pereira are the coordinators of the project and contributed with the manuscript corrections. Roberto F. M. Michel and Daniela Schmitz participated of the field work and contributed to data acquirement and analysis, and manuscript writing. Iorrana F. Sacramento, William F. Rodrigues and Caik O. de Miranda contributed to data analysis and manuscript writing.